Freestanding Single Crystalline Fe–Pd Ferromagnetic Shape Memory Membranes – Role of Mechanical and Magnetic Constraints Across the Martensite Transition

*Yanhong Ma, Annette Setzer, Jürgen W. Gerlach, Frank Frost, Pablo Esquinazi, and S. G. Mayr**

Substrate-attached and freestanding single crystalline $Fe_{70}Pd_{30}$ ferromagnetic shape memory alloy membranes, which were synthesized by molecular beam epitaxy on MgO (001) and later released from their substrates, are characterized with respect to their structural, thermal and magnetic properties. Residing in the two-phase region of austenite and the correct martensite phase with face centered tetragonal (fct) structure at room temperature, they reveal martensite transition with little hysteresis at 326 K and 320 K, respectively. Comparing substrate-attached with freestanding films, which show fundamentally different magnetic fingerprints, it is proposed that domain structure is capable of posing a bias on the austenite → fct-martensite phase transition by favoring martensite variants with their easy axis aligned along the field – just as the substrate constitutes a mechanical constraint on the transition. If confirmed, this would suggest thermo-magnetic actuation as an alternative where only moderate magnetic fields are feasible, but moderate temperature changes are possible.

1. Introduction

Due to their strong magneto-mechanical coupling, magnetic shape memory (MSM) alloys recently have attracted tremendous scientific interest as novel multiferroic material for actuator or strain sensor applications in microsystems.[1–5] In addition, they reveal all features of conventional shape memory alloys, such as superelasticity or the thermal shape memory effect.[6] While strain levels as high as almost 10% have been reported in Ni–Mn–Ga single crystals,[7] Fe–Pd based[2,6] thin films[8–11] and membranes[12–14] have attracted interest for complementary applications[15,16] that require higher corrosion resistance, lower brittleness and better biocompatibility.[2,17,18] In the latter, magnetically switchable strains up to 5% are attainable in presence of a single crystalline martensitic face centered tetragonal (fct) phase, while the competing body centered tetragonal (bct) and body centered cubic (bcc) martensite phases, as well as the face centered cubic (fcc) austenite ("γ" phase) need to be prevented.[6,19] Conveniently synthesized at elevated substrate temperatures within the austenite phase by molecular beam epitaxy (MBE) on MgO substrates,[9] the films need to transform to fct martensite before reaching the desired operating temperature and must be lifted-off the substrate to allow for motion of twin boundaries by relieving substrate constraints. While chemical-etching-based substrate lift-off, accompanied by post-annealing, recently has been demonstrated to yield the desirable fct martensite phase,[20] we have found in the present investigation that post-annealing can be omitted if a sufficiently high substrate temperature is employed during MBE.

The present contribution aims to give a thorough survey of the structural, thermal and magnetic properties of freestanding single crystalline Fe–Pd membranes, which reveal fundamentally different signatures than their substrate-attached counterparts. As possible explanation we propose, that – due to magneto-mechanical coupling – magnetic domain structure imposes a boundary condition to bias variant selection during austenite → martensite transition in freestanding films, which might prove to be of high relevance for alternative actuation concepts in future.

Y. Ma, Dr. J. W. Gerlach, Dr. F. Frost, Prof. Dr. S. G. Mayr
Leibniz-Institut für Oberflächenmodifizierung e.V. Permoserstrasse 15
D-04318 Leipzig, Germany
E-mail: stefan.mayr@iom.leipzig.de
Prof. Dr. S. G. Mayr
Translationszentrum für regenerative Medizin
Universität Leipzig, Germany
A. Setzer, Prof. Dr. P. Esquinazi, Prof. Dr. S. G. Mayr
Faculty of Physics and Earth Sciences
Institute for Experimental Physics II Universität Leipzig Linnéstr. 5,
04103 Leipzig, Germany

DOI: 10.1002/adfm.201103021

2. Results and Discussion

2.1. As Prepared Fe–Pd films on MgO (100) Substrates

Atomic force microscopy (AFM) measurements of 500 nm thick $Fe_{70}Pd_{30}$ single crystalline films grown on MgO (100) substrates (**Figure 1**a) unveil – besides crystalline facets – regular zig-zag type of surface modulations with a periodicity of 150–200 nm

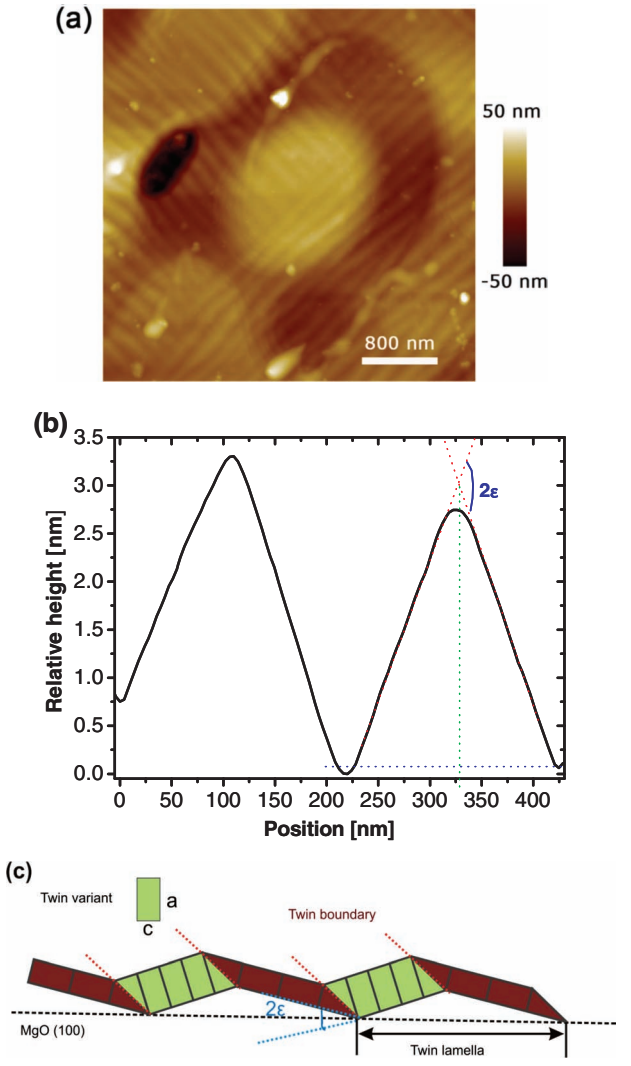

Figure 1. a) AFM surface topography of as-prepared martensitic Fe–Pd films on MgO (100) substrates and b) underlying structural model. The regular pattern arises from periodic repetition of two different adjoined martensite variants (c).

and a very moderate height of approx. 2.5 nm, as visualized in the characteristic height profile in Figure 1b. Typical for martensites,[21] this pattern is a direct manifestation of the underlying twin domain (often called "variant") structure, which forms under the influence of boundary conditions (viz. the attachment of the film to the substrate) under the premises of stress minimization upon cooling down. For the present system with a tetragonally distorted unit cell (with two long axes, *a* and one short axis, *c*) can either be aligned in plane or out of plane (Figure 1c); a modulation of these two variants (with twin boundaries in between) will thus be chosen by the system so as to minimize stress or, elastic energy after cooling through the austenite → martensite transition. From simple geometric considerations, the formula $\varepsilon = 45° - \arctan(c/a)$ is readily derived, which relates tetragonality, c/a, with the characteristic angle of the surface zig-zag profile, ε. As first suggested by Bain,[22] c/a can be used as order parameter to describe the transformation from face centered cubic 1 (fcc) to body centered cubic 0.707 (bcc) structure ("Bain path") with the two tetragonal phases, 0.94 (fct) and 0.72 (bct), in between. Averaging over 12 profiles, an angle of 1.6° is obtained from AFM measurements yielding a c/a ratio of 0.946, which indicates the film is in fct structure.

To quantify austenite ↔ martensite transition in substrate-attached films, temperature dependent X-ray diffraction (XRD(T)) and magnetization ($M(T)$) measurements were conducted. The XRD diffractograms (**Figure 2**a) of *as prepared* films at room temperature are characterized by one very sharp peak at 42.9° originating from the single crystalline MgO (100) substrate, while the other two peaks have to be attributed to austenite fcc (200) and martensite fct (200), viz. the films constitute a mixture of austenite and martensite phase. We focused our studies on the temperature dependence of the XRD for these (200) Bragg peaks in the following. When the temperature is increased to 308 K the fct (200) peak becomes weaker in intensity while the fcc peak is the dominating peak. Above 328 K, the film exhibits only a single fcc (200) reflection. As no other diffraction peaks are observed, this indicates that the film transfers from martensitic phase to austenitic phase completely at about 328 K, which we identify as austenite finish temperature. When subsequently decreasing temperature to room temperature, the fct (200) diffraction peak starts to grow, while the intensity of fcc (200) peak decreases reversibly. That is, the austenite transforms back to fct martensite during cooling. By further decreasing temperature down to 200 K, the fct peak keeps increasing in intensity, while the fcc peak becomes quite weak. Therefore, the films have a martensitic phase at 200 K with a small amount of austenite remainders, presumably located in proximity to the substrate, which suppresses transformations there. Within this context it is interesting to point out, that only one martensite fct (200) peak is observed at smaller angles than the fcc (200) peak, viz. only variants with the long *a*-axis perpendicular to the surface are favored during austenite → martensite transition

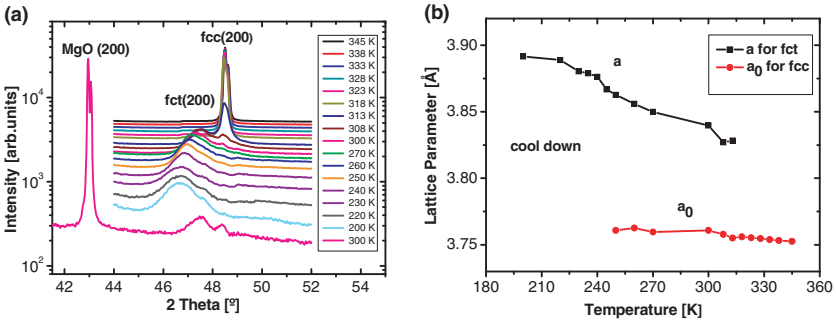

Figure 2. a) Austenite (fcc) to martensite (fct) phase transition in Fe–Pd films on MgO (100) observed by temperature dependent XRD measurements and b) corresponding lattice parameters. a_0 and a denote the cubic austenite and tetragonal martensite lattice parameters, respectively; both phases are present, were a_0 and a are given.

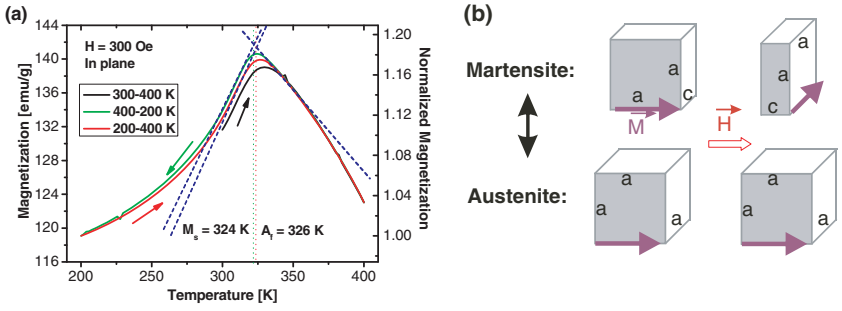

Figure 3. a) Temperature dependent magnetization measurements on martensitic Fe–Pd film on MgO (100) substrate. b) Sketch of martensite variants as well as austenite structures during $M(T)$ measurements.

and subsequent cooling down due to substrate constraints (growth stresses and differences in thermal expansion between Fe–Pd and MgO).[23] Furthermore, the temperature dependence of lattice parameters calculated from peak positions on cooling are plotted in Figure 2b. The lattice parameter a_0 of austenite remains almost constant during measurement presumably due to the invar properties of this alloy with an average value of 0.3757 ± 0.0001 nm, which agrees well with the literature value of 0.3752 nm for austenitic $Fe_{70}Pd_{30}$.[24] Tetragonality, on the other hand, increases with proceeding cooling, as indicated by an increase of a.

To independently confirm the above structure-based picture of a phase transition between austenite and a two-variant martensite phase with the short axis always aligned in-plane, we performed superconducting quantum interference device (SQUID) magnetometer measurements at moderate external fields aligned in-plane. All specimen were first heated up from room temperature to 400 K while applying a field as moderate as 300 Oe parallel to the sample surface. Then field cooling and field heating magnetization measurements with a temperature sweep rate of approx. 2 K min^{-1} were carried out ranging from 400 K to 200 K as shown in **Figure 3**a; arrows mark the direction of temperature variation. It is clearly visible that magnetization almost reversibly increases as a function of temperature up to ≈326 K, while following a decay above. While the latter is expected, we interpret the former in terms of the two-variant microstructure (Figure 3b), as saturation magnetizations of martensite and austenite have been demonstrated to differ only by a few percent[25] and thus cannot explain this observation: As in Fe–Pd fct martensite the easy axis of magnetization is the longer a axis,[26] shape anisotropy of the film enforces *in plane* magnetization and the external magnetic field is too weak to enforce reorientation, only half of the variants will have their magnetization directed parallel to the applied magnetic field deep in the martensite state. This changes dramatically during the martensite → austenite transition, where both variants equivalently become cubic with one of their three easy axes (and thus magnetization) directed along the locally applied field. While magnetic domain structure changes in favour for alignment of magnetization along the external field, this is reflected by an increasing magnetization in Figure 3a. It is worth emphasizing, that average magnetic domain structure almost reversibly changes back upon cooling-down, as indicated by only a slight hysteresis. From the location of maximum magnetizations, the martensite start temperature (M_s) and austenite finish temperature (A_f) are determined by the tangential method to be 324 K and 326 K, respectively. Consequently, the phase transformation temperature is confirmed by XRD(T) and SQUID independently to occur at about 326 K for the martensitic Fe–Pd thin films attached on MgO substrates.

2.2. Freestanding Fe–Pd Films

As a step towards an actuator, the films were released from the substrates by chemically dissolving the MgO substrate leaving crystal structure, phase and composition of these films intact.[20,27] From temperature dependent X-ray diffraction measurements (**Figure 4**a) it becomes obvious that until 320 K only fcc (200) and bcc/bct (110) peaks are observed, while upon cooling the fcc (200) peak splits into two peaks indexed as fct (200) and fct (002). We would like to emphasize, that occurrence of both peaks indicates presence of variants with their short axis aligned in plane and normal to the freestanding film, whereas substrate constraints prevent normal orientation in substrate attached films (Figure 2a). While we relate the bcc/bct peaks to the surface regions of the freestanding film,[28] Figure 4a clearly demonstrates presence of a reversible fcc-fct transformation. We would like to note that the intensities for freestanding films are much lower than for films on substrates–even upon ω optimization - due to buckling of the former. The corresponding lattice parameters (Figure 4b) at room temperature were determined to be: a = 0.3801 ± 0.0001 nm; c = 0.3626 ± 0.0001 nm for fct martensite, and a = 0.2955 ±0.0001 nm for bcc/bct, respectively. In fct martensite, the c/a ratio of 0.95 which is close to the c/a ratio estimated from AFM measurements while still attached on substrate (Figure 1). During cooling, the length

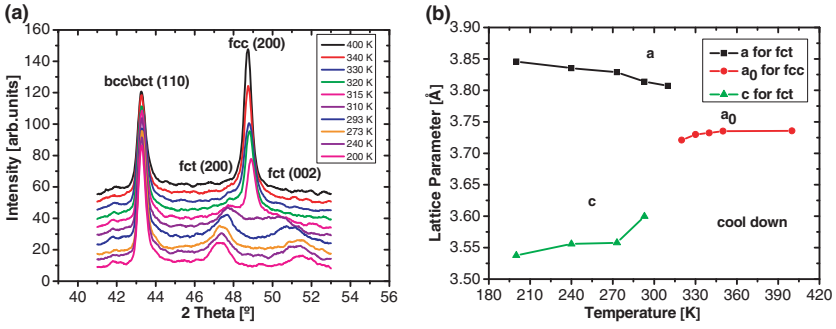

Figure 4. a) Austenite to fct-martensite phase transition in a freestanding film observed by temperature dependent XRD measurements and corresponding lattice parameters (b). a_0 and a /c denote the cubic austenite and tetragonal martensite lattice parameters, respectively; both phases are present, were a_0 and a/ c are given.

of the *a* and *c* axes decrease and increase gradually, respectively, corresponding to a decrease of the *c*/*a* ratio from 0.95 to 0.92. While martensite transition occurs around 320 K, the average lattice parameter a_0 for fcc austenite phase is determined to be around 0.3731 ± 0.0001 nm, which is less than for the film attached on MgO substrate.

Magnetization *M*(*T*) curves determined for martensitic freestanding thin films at external fields of 20 and 300 Oe, respectively (**Figure 5**a and b), show a more complex scenario: Magnetization exhibits a monotonic increase when heating the samples for the first time from room temperature up to 400 K, while remaining virtually constant after successive cooling and heating (demonstrated only for 300 Oe as shown in Figure 5b). To interpret these observations, it is instructive to relate *M*(*T*) to the XRD(*T*) measurements, as schematically sketched in Figure 5c. Based on X-ray diffraction (Figure 4a) all three martensite variants (1, 2 and 3) exist in this film at room temperature, while only two of these variants, e.g., 1 and 3, have one of their long crystallographic axes (the easy axes of magnetization) aligned parallel to the local magnetic field,[6] During martensite → austenite transformation in the course of heating, the symmetry changes from tetragonal to cubic; as all principal axes become easy axes of magnetization, domain structure changes in favor for increased parallel alignment of magnetization along the external field, viz. austenitic films reveal a higher apparent magnetization, basically similar to substrate-attached films (Section 2.1). However, when comparing these findings with the XRD(*T*) measurements discussed above (Figure 4a), it seems at first glance contradictory that the XRD(*T*) results show the phase transformation temperature at around 320 K, whereas the increase of magnetization can be still observed up to 400 K, i.e., within austenite. Two possible explanations can, in fact, account for this: Firstly, in presence of external fields as low as 300 Oe, the sample is still not revealing saturation magnetization (as also confirmed by the absolute magnetization levels), viz. a magnetic domain structure certainly will be present. Increase of magnetization with increasing temperature could thus result from thermally-assisted migration of domain boundaries (thermally activation across obstacles or motion due to reduced anisotropy at elevated temperatures). Secondly, increasing magnetization could also result from formation of pre-martensite (in the sense of fluctuations along soft-modes towards martensite) within austenite at these temperatures, which is influenced by the applied magnetic field. In fact, previous mechanical measurements have indicated presence of pre-martensite at these temperatures.[14] In any case, magnetization of freestanding films – when compared with substrate-attached films – shows strong signatures of de-pinning upon heating for the first time.

Upon cooling and further re-heating (demonstrated only for 300 Oe as shown in Figure 5b) magnetization continuously remains at an as elevated level as in austenite, while fingerprints of an austenite ↔ martensite phase transition are only very weak – like for substrate-attached films (Section 2.1) the austenite ↔ martensite transition also occurs at the absolute magnetization maximum, which is, however, much less pronounced for freestanding films. As all involved phases are known to reveal a comparable level of saturation magnetization,[24] these results strongly indicate absence of significant changes of the average magnetic domain structure during austenite ↔ martensite transition in freestanding films, in contrast to substrate-attached films, which reveal a greatly reversible evolution of domain structure upon heating and cooling. In the bottom line, presence and absence of substrate constraints correlate with irreversibility and reversibility of average magnetic domain structure, respectively. While for substrate-attached films, magnetic reversibility can readily be understood in terms of substrate-enforced structural reversibility, which transfers to magnetic structure via magneto-mechanical coupling, structural reversibility is lost in freestanding films. We assume, that when cooling-down austenite through the martensite transition, magnetic domain structure poses a bias in the sense that – in the absence of external boundaries – variants with their easy axis of magnetization aligned to the local field are preferred (Figure 5c). Thus magnetic domain structure could pose a boundary condition to bias selection of martensite variants in freestanding films, while mechanical boundaries enforced by substrate constraints dominate substrate-attached films. Clearly additional confirmation is necessary in future; this proposed scenario could, however, pave the way for thermo-mechanical switching with fields as low as some tens of Oe, as the latter can influence the domain structure. In particular

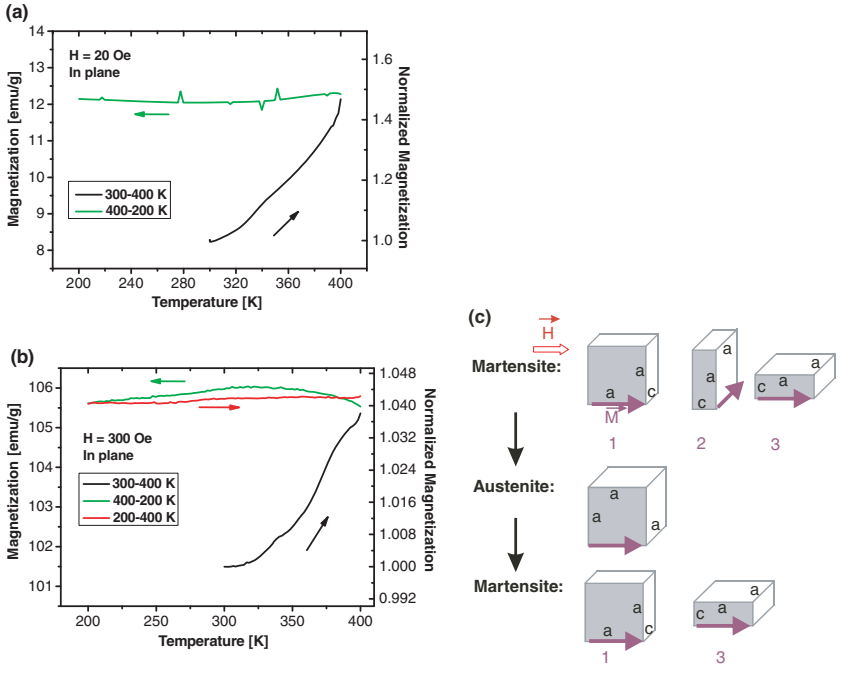

Figure 5. Temperature dependent magnetization measurements on martensitic freestanding Fe–Pd film with external magnetic field of a) 20 Oe and b) 300 Oe. c) Sketch of martensite variants as well as austenite structures during *M*(*T*) measurements.

when increasing sample temperature even beyond 400 K, viz. towards the Curie temperature. In view of typical switching fields in the range of some T required for reorientation of martensite variants in conventional MSM materials, this scenario thus would be highly exciting as it would provide novel thermomagnetic actuators switchable by several orders of lower magnetic fields as in the conventional MSM effect. As further confirmation and for exclusion of possible measuring artifacts, we prepared a purely austentic freestanding single crystalline film by MBE at a slightly lower deposition temperature, which – according to this interpretation – should not reveal this effect; this, in fact, is confirmed in **Figure 6**. For the sake of completeness we evaluated the Curie temperatures (T_C) for this austenitic freestanding film according to Kuz'min's model.[29] The parameters $ß = 1/3$, $p = 5/2$ and shape parameter $s = 1$ were kept constant to determine T_C by a fit of the relative magnetization curves,[13] yielding 677 K which is close to the T_C value of 600 K for bulk samples reported in the literature.[30,31] The slight difference might be due to the deviations from the Kuz'min's model fit by employing constant parameters $ß$, p and shape factor s.

3. Conclusions

To conclude, we characterized and compared the structural, magnetic and thermal properties of substrate-attached and freestanding single crystalline $Fe_{70}Pd_{30}$ thin films, which were prepared without post-annealing treatment by MBE at substrate temperatures of 1120 K or higher, subsequently quenched and later released from the substrate. As observed in XRD(T) measurements and – for the first time - AFM surface topographies, these films reside at room temperature in the two-phase region of fct-martensite and austenite. The fct-martensite ↔ austenite transition temperatures were detected to be 326 K and 320 K with little hysteresis for substrate-attached and freestanding films, respectively, as determined from XRD(T) and – for substrate-attached films – by temperature dependent SQUID magnetization measurements. To interpret the results, we propose that austenite → martensite transition in freestanding films is susceptible to magnetic domain structure, which poses an external boundary – just as mechanical constraints for substrate-attached films. These concepts could pave the way for employing Fe–Pd based membranes as magneto-thermal actuator in integrated devices, where magnetic fields as large as some Tesla (as required by the conventional MSM effect) are unavailable, but heating e.g., by directing electric current through the membrane is no great challenge.

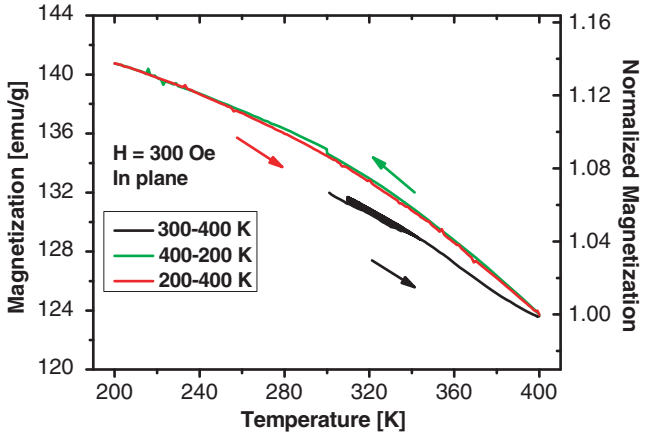

Figure 6. Temperature dependent magnetization measurements on austenitic freestanding Fe–Pd films.

4. Experimental Section

Single crystalline $Fe_{70}Pd_{30}$ thin films with 500 nm thickness were deposited onto MgO (100) substrates at 1120 K by molecular beam epitaxy (MBE) using ultra high vacuum (UHV) conditions (base pressure better than 10^{-9} mbar) as described before.[8,9,18] The films discussed presently were grown in the equilibrium γ phase (disordered fcc, austenite) with a total rate of about 0.15 nm s^{-1} from two independently rate-controlled electron beam evaporators. After deposition, samples were cooled down fast enough to suppress decomposition into stable, ordered $L1_0$ phase ($Fe_{50}Pd_{50}$) and α-Fe with the help of a surrounding liquid nitrogen cryo shield.[18] A saturated sodium bicarbonate solution was used to lift the films off their substrates, leaving the film structurally, morphologically and chemically intact; more details about the film deposition and lift-off procedures were described previously.[20] For all films energy-dispersive x-ray spectroscopy (EDX) using a Zeiss Ultra 55 field emission scanning electron microscope) was employed to verify the chemical composition before and after lift-off. Thin film surface topographies were characterized with a resolution of 1024 × 1024 pixels by atomic force microscopy (AFM–Bruker Dimension Icon AFM using Olympus AC160TS cantilevers with a nominal tip radius of 7 nm) in tapping mode. Temperature dependent XRD measurements from 200 K to 400 K employed a two-circle, URD 63 diffractometer (Seifert-FPM) equipped with a vacuum chamber (HDK S1, Buehler, Germany) with a base pressure better than 5×10^{-5} mbar to prevent condensation of humidity/ ice formation at low temperatures. The XRD patterns were recorded from 41° to 53° (2θ) with a step width of 0.01°. During measurements, the desired temperatures between 200 K and 400 K were obtained by balancing liquid nitrogen flow and output power of a resistive heater underneath the substrate (using a REP 1800 heating controller). Temperature dependent magnetization measurements (200 K to 400 K; temperature sweep rate approx. 2 K min^{-1}) were performed by a superconducting quantum interference device (SQUID) magnetometer MPMS-7 from Quantum Design in presence of an in-plane external magnetic field of 300 Oe and 20 Oe, respectively. While the films atop of substrates were cut into 5 mm x 5 mm pieces by a wafer-saw and mounted in a plastic straw of 5 mm diameter directly, freestanding films were fixed on a stick, which was subsequently inserted into the straw. The phase-transformation temperature was determined by the tangent method.

Acknowledgements

The authors thank F. Szillat for experimental assistance during film preparation, Dr. D. Manova and P.D. Dr. S. Mändl for XRD(T) measurements prior to the present work as well as Prof. Dr. Dr. h.c. B. Rauschenbach for general support. We gratefully acknowledge financial supports in parts from the Leipzig Graduate School of Natural Sciences "Building with Molecules and Nano Objects" (BuildMoNa) through the German Science Foundation (DFG), as well as the German Federal Ministry of Education and Research (BMBF, PtJ-BIO, 0315883).

Received: December 14, 2011
Published online: March 22, 2012

[1] K. Ullakko, J. K. Huang, C. Kantner, R. C. O. Handley, V. V. Kokorin, *Appl. Phys. Lett.* **1996**, *69*, 1966.
[2] R. D. James, M. Wuttig, *Philos. Mag. A* **1998**, *77*, 1273.
[3] J. W. Dong, L. C. Chen, C. J. Palmstrom, R. D. James, S. McKernan, *Appl. Phys. Lett.* **1999**, *75*, 1443.
[4] R. Kainuma, Y. Imano, W. Ito, Y. Sutou, H. Morito, S. Okamoto, O. Kitakami, K. Oikawa, A. Fujita, T. Kanomata, K. Ishida, *Nature* **2006**, *439*, 957.
[5] C. A. Jenkins, R. Ramesh, M. Huth, T. Eichhorn, P. Porsch, H. J. Elmers, G. Jakob, *Appl. Phys. Lett.* **2008**, *93*, 234101.
[6] J. Cui, T. W. Shield, R. D. James, *Acta Mater.* **2004**, *52*, 35.
[7] A. Sozinov, A. A. Likhachev, N. Lanska, K. Ullakko, *Appl. Phys. Lett.* **2002**, *80*, 10.
[8] I. Kock, T. Edler, S. G. Mayr, *J. Appl. Phys.* **2008**, *103*, 046108.
[9] L. Kühnemund, T. Edler, I. Kock, M. Seibt, S. G. Mayr, *New J. Phys.* **2009**, *11*, 113054.
[10] J. Buschbeck, I. Opahle, M. Richter, U. Rößler, P. Klaer, M. Kallmayer, H. J. Elmers, G. Jakob, L. Schultz, S. Fähler, *Phys. Rev. Lett.* **2009**, *103*, 216101.
[11] J. Buschbeck, S. Hamann, A. Ludwig, B. Holzapfel, L. Schultz, S. Fähler, *J. Appl. Phys.* **2010**, *107*, 113919.
[12] I. Kock, S. Hamann, H. Brunken, T. Edler, S. G. Mayr, A. Ludwig, *Intermetallics.* **2010**, *18*, 877.
[13] S. Hamann, M. E. Gruner, S. Irsen, J. Buschbeck, C. Bechtold, I. Kock, S. G. Mayr, A. Savan, S. Thienhaus, E. Quandt, S. Fähler, P. Entel, A. Ludwig, *Acta Mater.* **2010**, *58*, 5949.
[14] I. Claussen, S. G. Mayr, *New J. Phys.* **2011**, *12*, 063034.
[15] M. Kohl, D. Brugger, M. Ohtsuka, T. Takagi, *Sens. Actuators A* **2004**, *114*, 445.
[16] C. Bechtold, I. Teliban, C. Thede, S. Chemnitz, E. Quandt, *Sens. Actuators A* **2010**, *158*, 224.
[17] T. Kakeshita, T. Fukuda, *Mater. Sci. Forum* **2002**, *394*, 531.
[18] Y. Ma, M. Zink, S. G. Mayr, *Appl. Phys. Lett.* **2010**, *96*, 213703.
[19] M. Matsui, H. Yamada, K. Adachi, *J. Phys. Soc. Jpn.* **1980**, *48*, 2161.
[20] T. Edler, S. G. Mayr, *Adv. Mater.* **2010**, *22*, 4969.
[21] P. Leicht, A. Laptev, M. Fonin, Y. Luo, K. Samwer, *New J. Phys.* **2011**, *13*, 033021.
[22] E. C. Bain, *Trans. Am. Inst. Min. Metall. Pet. Eng.* **1924**, *70*, 25.
[23] T. Edler, J. Buschbeck, C. Mickel, S. Fähler, S. G. Mayr, *New J. Phys.* **2008**, *10*, 063007.
[24] M. Foos, C. Frantz, M. Gantois, *J. Phys.* **1982**, *43*, C4-389.
[25] S. G. Mayr, *Phys. Rev. B* **2012**, *85*, 014105.
[26] J. Cui, R. D. James, *IEEE Trans. Magn.* **2001**, *37*, 2675.
[27] T. Edler, S. Hamann, A. Ludwig, S. G. Mayr, *Scripta Mater.* **2011**, *64*, 89.
[28] During film growth, the first layers on the MgO substrate grow as Fe and $L1_0$ $Fe_{50}Pd_{50}$,[9] which are still present in the freestanding films. These layers in addition act as nucleation site for the bcc/bct martensite phase; hence, the bcc/bct peak is observed.[8]
[29] M. D. Kuz'min, *Phys. Rev. Lett.* **2005**, *94*, 107204.
[30] A. Kussmann, K. Jessen, *J. Phys. Soc. Jpn.* **1962**, *17*, 136.
[31] M. Matsui, T. Shimizu, H. Yamada, K. Adachi, *J. Magn. Magn. Mater.* **1980**, *15*, 1201.